

Differential Activity and Structure of Highly Similar Peroxidases. Spectroscopic, Crystallographic, and Enzymatic Analyses of Lignifying *Arabidopsis thaliana* Peroxidase A2 and Horseradish Peroxidase A2^{†,‡}

Kåre Lehmann Nielsen,[§] Chiara Indiani,^{||} Anette Henriksen,^{⊥,Ⓢ} Alessandro Feis,^{||} Maurizio Becucci,[#] Michael Gajhede,[⊥] Giulietta Smulevich,^{*,||} and Karen G. Welinder^{*,§}

Institut for Biotechnologi, Aalborg Universitet, Sohngaardsholmsvej 49, DK-9000 Aalborg, Denmark, Dipartimento di Chimica, Università di Firenze, Via G. Capponi 9, I-50121 Firenze, Italy, Protein Structure Group, Department of Chemistry, University of Copenhagen, Universitetsparken 5, DK-2100 Copenhagen, Denmark, LENS-European Laboratory for Non Linear Spectroscopy, Largo Fermi 2, I-50125 Firenze, Italy, and Department of Chemistry, Carlsberg Laboratory, Gamle Carlsberg Vej 10, DK-2500 Valby, Denmark

Received April 2, 2001; Revised Manuscript Received July 23, 2001

ABSTRACT: Anionic *Arabidopsis thaliana* peroxidase ATP A2 was expressed in *Escherichia coli* and used as a model for the 95% identical commercially available horseradish peroxidase HRP A2. The crystal structure of ATP A2 at 1.45 Å resolution at 100 K showed a water molecule only 2.1 Å from heme iron [Østergaard, L., et al. (2000) *Plant Mol. Biol.* 44, 231–243], whereas spectroscopic studies of HRP A2 in solution at room temperature [Feis, A., et al. (1998) *J. Raman Spectrosc.* 29, 933–938] showed five-coordinated heme iron, which is common in peroxidases. Presented here, the X-ray crystallographic, single-crystal, and solution resonance Raman studies at room temperature confirmed that the sixth coordination position of heme iron of ATP A2 is essentially vacant. Furthermore, electronic absorption and resonance Raman spectroscopy showed that the heme environments of recombinant ATP A2 and glycosylated plant HRP A2 are indistinguishable at neutral and alkaline pH, from room temperature to 12 K, and are highly flexible compared with other plant peroxidases. Østergaard et al. (2000) also demonstrated that ATP A2 expression and lignin formation coincide in *Arabidopsis* tissues, and docking of lignin precursors into the substrate binding site of ATP A2 predicted that coniferyl and *p*-coumaryl alcohols were good substrates. In contrast, the additional methoxy group of the sinapyl moiety gave rise to steric hindrance, not only in A2 type peroxidases but also in all peroxidases. We confirm these predictions for ATP A2, HRP A2, and HRP C. The specific activity of ATP A2 was lower than that of HRP A2 (pH 4–8), although a steady-state study at pH 5 demonstrated very little difference in their rate constants for reaction with H₂O₂ ($k_1 = 1.0 \mu\text{M}^{-1} \text{s}^{-1}$). The oxidation of coniferyl alcohol, ferulic, *p*-coumaric, and sinapic acids by HRP A2, and ATP A2, however, gave modest but significantly different k_3 rate constants of 8.7 ± 0.3 , 4.0 ± 0.2 , 0.70 ± 0.03 , and $0.04 \pm 0.2 \mu\text{M}^{-1} \text{s}^{-1}$ for HRP A2, respectively, and 4.6 ± 0.2 , 2.3 ± 0.1 , 0.25 ± 0.01 , and $0.01 \pm 0.004 \mu\text{M}^{-1} \text{s}^{-1}$ for ATP A2, respectively. The structural origin of the differential reactivity is discussed in relation to glycosylation and amino acid substitutions. The results are of general importance to the use of homologous models and structure determination at low temperatures.

Horseradish root has been the traditional source of heme peroxidases (HRP,¹ EC 1.11.1.7). Several enzymes with acid,

[†] This research was supported by the EU Biotechnology Program "Towards Designer Peroxidases" BIO4-CT97-2031 (to M.G., G.S., and K.G.W.), Italian CNR, and MURST Cofin (to G.S.).

[‡] Coordinates and structure factors for ATP A2 at room temperature have been deposited in RCSB Protein Data Bank as entry 1Q04.

* To whom correspondence should be addressed. G.S.: telephone, (+39)055-2757596; fax, (+39)055-2476961; e-mail, smulev@chim.unifi.it. K.G.W.: telephone, (+45)9635-8467; fax, (+45)9814-1808; e-mail, welinder@bio.auc.dk.

[§] Aalborg Universitet.

^{||} Università di Firenze.

[⊥] University of Copenhagen.

[Ⓢ] Carlsberg Laboratory.

[#] LENS-European Laboratory for Non Linear Spectroscopy.

¹ Abbreviations: ATP, *A. thaliana* peroxidase; HRP, horseradish peroxidase; SBP, soybean peroxidase; BP, barley grain peroxidase; cpd, compound or intermediate of enzymatic reaction; HS, high-spin; LS, low-spin.

neutral, and very high isoelectric points have been purified (1–3). All reacted with a wide range of substrates. Isoenzyme C, HRP C, with a pI of 8.8 accounts for ~50% of the activity in the root and has found a number of practical applications, in coupled enzyme assays for diagnostic analyses or in visualization of immune reactions. HRP C was the first peroxidase to be sequenced (4), and it has been analyzed extensively in its recombinant form (5). The catalytic and spectroscopic properties of HRP C have been further elucidated by the study of many mutants (6–8). The structure of HRP C has been determined (9), and the structures of the HRP C–ferulic acid and the ternary HRP C–ferulic acid–CN complexes have also become available (10).

HRP A2, with a pI of 3.5, is the most abundant anionic peroxidase from horseradish root. Although its specific activity is generally lower than that of HRP C, it is an interesting isozyme, since it is less readily inactivated by

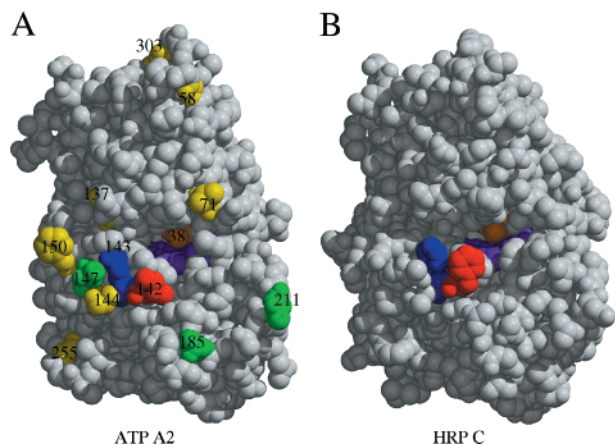


FIGURE 1: Structures of ATP A2 and HRP C. (A) A space-filling model of the surface of recombinant ATP A2 is viewed toward the substrate access channel (20). The heme (violet) is oriented horizontally with the N-terminal or distal domain above. The catalytic Arg38 is orange. The residues that differ between ATP A2 and HRP A2 are yellow. All are accessible at the surface and, therefore, not supposed to affect the interior packing of the A2 enzymes. The asparagine residues glycosylated in plant HRP A2 are highlighted in green (17) (EMBL accession number P80679). The same residues are predicted to be glycosylated in plant ATP A2 (together with two extra sites at Asn135 and -303). These bulky glycans are absent in the recombinant ATP A2 expressed in *E. coli*. The glycan at Asn147 and the Ile142Phe substitution near the substrate access channel are proposed to affect the substrate binding at the heme edge. (B) The surface of HRP C is shown in the same orientation. Phe142 (red) is found also in HRP A2 but is substituted with Ile in ATP A2. Phe143 (blue) is substituted with Glu in both A2 enzymes. The glycan at Asn147 is absent in HRP C.

peroxides (11, 12). The enzymatic, ligand-binding, redox (11), NMR (13, 14), electronic absorption, resonance Raman, and EPR (15, 16) properties of HRP A2 have been extensively studied and compared to those of HRP C. The amino acid sequence of HRP A2 has been determined using an enzyme preparation provided by I. Yamazaki (17; EMBL accession number P80679). The amino acid sequence of HRP A2 is 53% identical to that of HRP C. HRP A2 carries seven N-linked glycans, which show the same structure and heterogeneity as the eight glycans of HRP C (18). The major glycan form has the structure Man α 3(Man α 6)(Xyl β 2)-Man β 4GlcNAc β 4(Fuc α 3)GlcNAc-. Homogeneity of HRP A2 could be significantly increased by treatment with α -mannosidase, but crystallization was not successful (K. Teilum, A. Henriksen, M. Gajhede, and K. G. Welinder, unpublished data). A small amount of the orthologous, 95% identical ATP A2 peroxidase had previously been purified from a cell suspension culture of *Arabidopsis thaliana*, and cloned from the same source (19). A recombinant form of the mature ATP A2 was produced as a model for plant HRP A2 and crystallized. The structure was determined to 1.45 Å resolution at 100 K (20), and was found to be very similar to the structure of HRP C (Figure 1). However, the ATP A2 structure showed water bound to the heme Fe at a distance of only 2.1 Å at the sixth coordination position. A ligand distance of 2.1 Å might influence peroxidase activity and is in conflict with the largely five-coordinate heme iron observed at room temperature for HRP A2 (15). Østergaard et al. (20) further showed that ATP A2 gene expression coincides with lignification, and predicted that among the lignin precursors only coniferyl and *p*-coumaryl, but not

sinapyl alcohol, would bind well at the substrate binding site of peroxidases.

Consequently, the present state of knowledge leaves us with three major questions. First, is ATP A2 a valid model for HRP A2 in terms of structure and enzymatic properties? Second, is the crystal structure at 100 K a valid model for the active site of ATP A2 at room temperature? Third, docking studies have predicted that some lignin precursors react preferentially with peroxidases; can this be confirmed? These questions have been addressed by spectroscopic comparisons of the recombinant ATP A2 and the plant HRP A2 from room temperature to 12 K, single-crystal resonance Raman spectroscopy and X-ray crystallography of ATP A2 at room temperature, and comparison of enzymatic activities of ATP A2, HRP A2, and HRP C.

MATERIALS AND METHODS

Recombinant ATP A2. The cDNA, encoding a signal peptide in front of the mature peroxidase, was modified to encode only the 305-residue mature protein with an initiating Met and two stop codons. This gene was inserted between the *Nde*I and *Bam*HI sites in the pET-3a vector (the recombinant ATP A2 contains this Met as shown by amino acid sequencing, but it is counted as residue 0) (20). The *atpA2*-containing plasmid was expressed in *Escherichia coli* BL21(DE3pLysS) (21) in 3 L batches in a fermentor (Aplikon) at 37 °C. Oxygen was supplied by bubbling compressed air (4 psi) through the fermentation medium (2 \times YT), and stirring was fixed at a rate of 1000 rpm. Expression was induced by addition of isopropyl thiogalactoside to a final concentration of 0.4 μ M at an OD₆₀₀ of 0.8. After 4 h, the cells were harvested by centrifugation. Inclusion bodies were isolated, washed, and dissolved according to the method described in ref 22. Active ATP A2 was obtained by diluting the denatured protein to a final concentration of 20 μ g/mL in 20 mM Tris-HCl (pH 8.5), 0.4 mM reduced and 0.6 mM oxidized glutathione, 1.5 μ M hemin chloride, 6 mM CaCl₂, and 1.2 M urea at 8 °C. After 16 h, the folding solution was concentrated 500-fold and dialyzed against 2.5 mM Tris-HCl (pH 8.3) and 0.25 mM CaCl₂. Significant purification was achieved by removing the precipitated protein by centrifugation. Soluble peroxidase was filtered and subjected to chromatography, at first on HiLoad Q-Sepharose at pH 8.3, and then on MonoQ (20). The resulting fraction was precipitated by adding ammonium sulfate to a final concentration of 2.5 M, and stored at 4 °C.

Benzohydroxamic Acid Affinity Chromatography. ATP A2 was retained on benzohydroxamic acid agarose (KemEnTec) at a slow flow rate in 50 mM sodium phosphate and 1 mM CaCl₂ at pH 5.0 (23), as shown previously for HRP A2 (24). The protein was eluted isocratically in the same buffer, and the activity peak was concentrated by ultrafiltration (Centricon 10, Amicon). The absorption spectrum gave an RZ (Reinheitszahl) value A_{403}/A_{280} of 4.1 and showed the complete absence of any low-spin heme.

HRP A2 was purchased from Biozyme (batch 898 DX; A_{403}/A_{280} = 3.75) in a freeze-dried form and used without further purification, since MonoQ chromatography and SDS-PAGE indicated homogeneity.

HRP C was purified from type II peroxidase (Roche) by chromatography on S-Sepharose in 5 mM NaAc buffer (pH

4.7) by applying a gradient of NaCl. The major peak was rechromatographed. Further purification was achieved by benzohydroxamic acid affinity chromatography as described above, giving HRP C with an A_{403}/A_{280} ratio of 3.1 (24).

Spectroscopic Analyses in Solution and Single Crystals. The ATP A2 and HRP A2 proteins were dissolved in either 0.1 M bicine [*N,N*-bis(2-hydroxyethyl)glycine] at pH 7.5, or 0.1 M phosphate at pH 7.0, for the neutral pH solution experiments. The alkaline form was obtained in 0.1 M glycine buffer at pH 10.5. Protein concentrations were 30–150 μ M for both electronic absorption and RR spectroscopy at room temperature (15 °C), and 14–150 μ M for electronic absorption and 180–200 μ M for RR spectra for the low-temperature measurements. The experiments in solution were carried out as previously described for HRP A2 (15, 16).

For single-crystal experiments, ATP A2 crystals were placed with a small amount of mother liquor on a slide and the slide was sealed by vacuum grease with a cover glass, or mounted with a small amount of mother liquor in a 0.6 mm capillary which was then sealed. The Raman microprobe apparatus described previously (25) was further improved. The microscope was equipped with an extralong working distance Nikon M Plan achromatic objective capable of 60 \times magnification with a 0.70 numerical aperture. The laser beam waist in the focus of the objective was ~ 2 μ m. The spectrometer was an HR460 Jobin-Yvon monochromator with a grating of 1800 grooves/mm and an ultimate resolving power exceeding 10^4 at 550 nm. To attenuate the strong Rayleigh scattering, a notch filter (Kaiser Optical Systems Holographic SuperNotch) was inserted in the optical path. The detector was a liquid nitrogen-cooled Spectraview 2D CCD head of 578×375 pixels allowing the simultaneous recording of a spectral region of 450 cm^{-1} with the present grating. The 200 μ m slit gave 5 cm^{-1} spectral resolution and a reasonable signal-to-noise ratio. The spectra were obtained with excitation from the 514.5 nm line of an Ar⁺ laser (Coherent Innova/90), with a power of 50 μ W on the crystal surface. The grating of the spectrometer was fixed during the experiment, and the spectra were calibrated with indene as a standard. The frequencies were accurate to $\pm 1\text{ cm}^{-1}$ for the intense isolated bands and to approximately $\pm 2\text{ cm}^{-1}$ for overlapping bands and shoulders.

Crystallization of ATP A2 and Crystallography at Room Temperature. Crystals of ATP A2 were obtained in 0.1 M Mg(CH₃COO)₂, 0.5 M cacodylate (pH 6.5), and 10% (w/v) PEG 8000 (20). A crystal was mounted in a capillary, and diffraction data were collected at room temperature using 2° oscillations. A Rigaku R-axis IIC image plate system with a Rigaku RU200 rotating anode supplied the Cu K α X-ray beam at 50 kV and 180 mA. The crystal to detector distance was 90 mm, and the exposure time was 60 min for each frame. The unit cell was primitive orthorhombic $P2_12_12_1$ with the following cell dimensions: $a = 32.3\text{ \AA}$, $b = 74.2\text{ \AA}$, and $c = 119.5\text{ \AA}$ with a mosaicity of 0.25°. The diffraction limits of the ATP A2 crystals were 3.0 \AA under these conditions. A complete model of ATP A2 determined at 100 K to 1.45 \AA resolution (PDB entry 1PA2) was used for structure determination by molecular replacement. After an initial simulated annealing to 4500 K, the following CNS (26) runs included only positional refinement. The B -factors were fixed at 15 \AA^2 as the refinement of B -factors resulted in nonphysical low values. Solvent was included in the model

Table 1: Statistics for Crystallographic Structure Determination of ATP A2 at Room Temperature

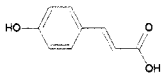
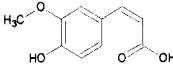
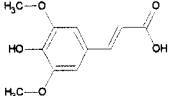
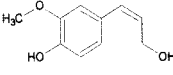
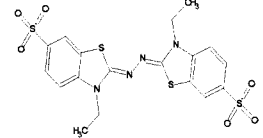
data collection	
resolution range (\AA)	30–3.0
no. of observations	27478
no. of unique reflections	5887
completeness (%) ^a	97.8 (97.3)
$I/\sigma I$	15.0 (4.5)
R_{sym} (%) ^{a,b}	16.5 (29.5)
refinement	
resolution range (\AA)	30–3.0
no. of unique reflections ($I > 0$)	5867
R_{cryst} (%) ^c	0.183 (0.220)
R_{free} (%) ^d	0.235 (0.371)
no. of non-hydrogen atoms	
protein	2249
1 heme and 2 Ca ²⁺	45
solvent	68
rms deviations from ideal values	
bond lengths (\AA)	0.008 ^e
bond angles (deg)	1.3 ^e
estimated mean coordinate error (\AA)	
SigmaA	0.29 ^e
Luzzati plot	0.26 ^e
Ramachandran plot ^f	
residues in most favored (disallowed) regions (%)	89.6 (0.0)

^a Numbers in parentheses are for the highest-resolution shell (3.11–3.00 \AA). ^b $R_{\text{sym}} = \sum_{hkl} (\sum_i (|I_{hkl,i}| - \langle I_{hkl} \rangle)) / \sum_{hkl,i} |I_{hkl,i}|$, where $I_{hkl,i}$ is the intensity of an individual measurement of the reflection with Miller indices h , k , and l , and $\langle I_{hkl} \rangle$ is the mean intensity of that reflection. ^c $R_{\text{cryst}} = \sum_{hkl} (|F_o| - |F_c|) / \sum_{hkl} |F_o|$, where $|F_o|$ and $|F_c|$ are the observed and calculated structure factor amplitudes. ^d R_{free} is equivalent to the R -factor, but calculated with reflections omitted from the refinement process (5% of reflections omitted). ^e Calculated with the program CNS (26). ^f Calculated with the program PROCHECK (45).

despite the relatively low resolution of the data. A lowering of R_{free} (5% of the reflections used for R_{free} determination) by 2.4% and the presence of excess $2F_o - F_c$ electron density in appropriate positions justified this. A $3\sigma F_o - F_c$ electron density appears with a center 2.5 \AA above the heme iron and 3.5 \AA from H42 N_{E2} after the final refinement. A water molecule was not fitted into this density as no positive $2F_o - F_c$ density is returned after additional refinement. The presence of this density indicates a partially occupied water position 2.5 \AA above the heme iron. With 3 \AA resolution data, the occupancy could not be refined and this water position is omitted from atomic coordinates. The final R -factor of the model is 18.3%, while R_{free} is 23.5%, including 68 solvent molecules. The room-temperature atomic coordinates and structure factors for ATP A2 were deposited in the Protein Data Bank as entry 1Q04. Data collection and refinement statistics are summarized in Table 1.

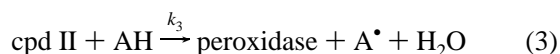
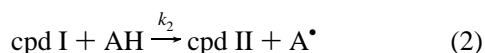
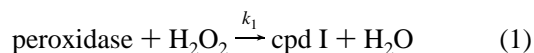
Peroxidase Activity. Ferulic acid, coniferyl alcohol, *p*-coumaric acid, sinapic acid, and 2,2'-azinobis(3-ethylbenzothiazoline-6-sulfonic acid) (ABTS) were purchased from Sigma. Substrate and product properties are summarized in Table 2. Absorption spectra of substrates and products of *p*-coumaric acid and sinapic acid were recorded at pH intervals of 0.5 from pH 4 to 8, and extinction coefficients were determined according to the method described in ref 27. Activity measurements were monitored at 290 nm for *p*-coumaric acid and at 308 nm for sinapic acid, i.e., the isosbestic points of these substrates, pH 4–8. The consumption of substrates was monitored, except for ABTS where the formation of the stable radical product was monitored (28). The concentration of hydrogen peroxide was determined

Table 2: Properties of Peroxidase Substrates

Hydrogen donor	Coumaric acid	Ferulic acid	Sinapic acid	Coniferyl alc.	ABTS
Structure					
pK _a	4.4, 8.8	4.4, 9.0	4.4, 8.6	9.4	
Wavelength, nm	308 290	318 310	308	264	340 414
ε _{substrate} , mM ⁻¹ cm ⁻¹	19.2 26.3	15.2 16.0	21.3	14.8	36 0
ε _{product} , mM ⁻¹ cm ⁻¹	7.5 14.7	6.0 7.32	7.0	6.6	36
Δε, mM ⁻¹ cm ⁻¹	11.7 11.6	9.2 8.68	14.3	8.2	36
Reference	(46)	(27, 30)	This study	(27)	(28)
	This study				

from the ϵ_{240} of 43.6 M⁻¹ cm⁻¹. All substrates were freshly made before use. Buffers were 50 mM sodium citrate at pH 4.0 and 5.0, 50 mM 2-morpholinoethanesulfonic acid (MES) at pH 6.0 and 7.0, and 4-(2-hydroxyethyl)piperazine-1-ethanesulfonic acid (HEPES) at pH 8.0. All contained 1 mM CaCl₂. Enzyme was dissolved in 2.5 mM MES and 0.1 mM CaCl₂ (pH 7) at 11 times the final assay concentration. Peroxidase concentrations were determined using an ϵ of 100 mM⁻¹ cm⁻¹ at the Soret peak maximum at 403 nm (this rule is generally applicable for the normally five-coordinated heme peroxidases measured at neutral pH in 10 mM nonbinding buffer). Final concentrations were 1–15 nM enzyme, 136 μ M reducing substrate, and 500 μ M H₂O₂. Reactions were assessed using the SX-18MV stopped-flow instrument (Applied Photophysics) at 25 ± 0.2 °C. Injections of 10 volumes of substrate in buffer for 1 volume of enzyme solution were used. Data collection was initiated immediately (~20 ms after mixing) and continued for 10–50 s. Initial rates were determined from at least five injections. The activity is reported as moles of reducing substrate turned over per mole of enzyme per second. Units of micromolar per milligram per minute can be obtained by multiplying by 1.4 for the glycosylated HRP A2 and HRP C (43 kDa) and by 1.7 for the recombinant nonglycosylated ATP A2 (35 kDa).

Determination of Rate Constants. Peroxidases follow a three-step reaction cycle (29):



In the catalytic cycle, 1 mol of hydrogen peroxide oxidizes

2 mol of hydrogen donor into radicals ($\text{H}_2\text{O}_2 + 2\text{AH} \rightarrow 2\text{A}^\bullet + 2\text{H}_2\text{O}$). In most cases, $k_2 \gg k_3$, and $k_2k_3/(k_2 + k_3)$ approaches k_3 . Under steady-state conditions, we obtain $(d[\text{AH}]/dt)/2[\text{E}]_0 = k_3[\text{AH}][\text{H}_2\text{O}_2]/[(k_3/k_1)[\text{AH}] + [\text{H}_2\text{O}_2]]$ (27, 29, 30). The rate constants k_1 and k_3 were estimated for ATP A2 and HRP A2 at pH 5.0 using the same buffer as above and varying the H₂O₂ concentration from 2 to 1000 μ M at 7.5–60 nM enzyme and 136 μ M reducing substrate. Experiments were carried out using the SX-18MV stopped-flow instrument from Applied Photophysics. Initial rates were plotted as a function of the concentration of H₂O₂ and the data fitted to the rate equation by nonlinear regression using KaleidaGraph version 3.5 (Synergy Software).

RESULTS AND DISCUSSION

Recombinant *A. thaliana* Anionic Peroxidase, ATP A2. ATP A2 protein was originally isolated, microsequenced, and cloned from an *Arabidopsis* root-cell suspension culture (19) (GenBank accession number X99952). Recombinant ATP A2 was previously obtained by expression in *E. coli* BL21-(DE3) followed by in vitro folding from inclusion body protein (20). However, the expression yield was very low compared to those previously obtained for recombinant barley grain peroxidase BP 1, neutral *A. thaliana* peroxidase, ATP N (22), and soybean seed coat peroxidase SBP (31). Therefore, it appeared that the *atpA2* gene product might be toxic to the cell due to the well-known leaky expression of the T7 promoter system prior to induction. An effort to enhance expression by regulating the expression of T7 polymerase, using the AraBAD promoter, gave a significant increase in the level of T7 polymerase expression upon induction with L-arabinose, but failed to increase the yield of the ATP A2 polypeptide. In contrast, expressing ATP A2 in BL21(DE3pLysS) (21) resulted in a level of expression of approximately 60 mg/L of fermentation broth, at least 10-

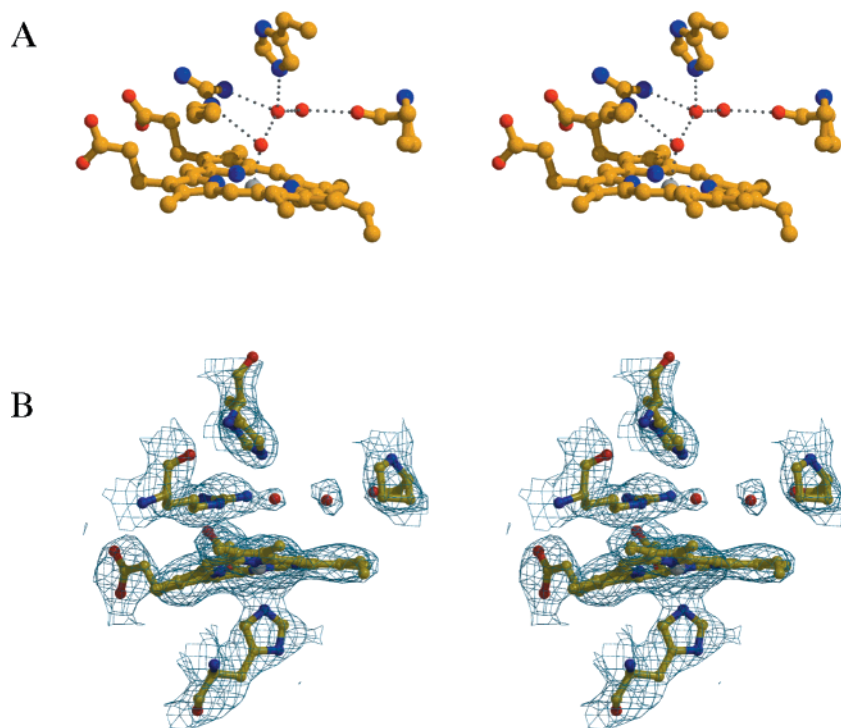


FIGURE 3: Active site of ATP A2 as observed by X-ray crystallographic analyses. (A) Data collection at 100 K and 1.45 Å resolution (20). Important distal residues conserved in all peroxidases (Arg38, His42, and Pro138), are shown together with three water molecules. Dashed lines denote hydrogen bonds between water molecules and amino acid residues, inferred on the basis of distance criteria (2.4–3.0 Å) (see the text). The distance between the Fe atom and the distal water molecule is 2.1 Å. (B) Data collection at room temperature giving 3.0 Å resolution. The 1σ $2F_o - F_c$ electron density in the heme cavity of ATP A2 at room temperature, before water was included in the refinement.

to crystal I. They are due to the presence of a small amount of 6-c LS heme as judged by the comparison with the spectrum of ATP A2 at pH 10.5 (Figure 4e), which is a pure 6-c LS form. The difference between crystals I and II was not induced by the crystallization medium, since the spectrum of ATP A2 dissolved in the medium (Figure 4a) gave rise to a spectrum almost identical to the one in bicine at pH 7.5. We can also exclude that the spectrum was an artifact induced by the heating of the crystal by the laser beam, since no damage was detected on the surface of the crystals after irradiation with the very low power applied, and no spectral changes were observed during the exposure time. The experimental conditions giving rise to the slightly different crystal spectra are not clear, but crystal II demonstrates that it is possible to induce the formation of a 6-c LS heme in ATP A2 even at room temperature, confirming the presence of a flexible distal side.

In conclusion, the RR data show that the heme environments of ATP A2 and HRP A2 are indistinguishable under all experimental conditions, and together with the crystallographic data confirm that the predominant form of ATP A2 is a 5-c QS heme at neutral pH and room temperature. Therefore, the sixth coordination position of the heme iron of these homologues is essentially vacant and accessible to the reaction with hydrogen peroxide under physiological conditions.

Enzyme Activity. ATP A2 expression in *Arabidopsis* plants is closely linked to lignin formation *in vivo* (20). Since lignin of a typical angiosperm is composed of coniferyl, sinapyl, and *p*-coumaryl alcohol (approximately 100:70:7) (36), it was of obvious interest to predict the substrate preference of ATP A2 toward these alcohols by docking the molecules into the

high-resolution structure of ATP A2. The docking showed that coniferyl and *p*-coumaryl alcohol fitted well at the site of ferulic acid binding [observed in HRP C (10)]. In contrast, the additional methoxy group of the sinapyl or sinapic moiety (chemical structures in Table 2) overlapped with the main chain CO of Pro139, and would be sterically hindered from the primary site of substrate binding. This prediction was suggested to be general for all plant peroxidases because Pro139 is conserved (37, 38). Here we show that the prediction of monolignol substrate specificity is correct for ATP A2, HRP A2, and HRP C (Table 3).

For practical reasons, we used the more stable and commercially available corresponding acids for substrates. The carboxylic acid groups have a pK_a of 4.4 for these substrates (Table 2). In the study presented here, we have selected buffers that are expected not to be inhibitory (in contrast with acetate, nitrate, ammonia, and Tris that can bind to the substrate-binding site in several peroxidases). Table 3 compares the turnover of ferulic, *p*-coumaric, and sinapic acid by HRP A2, ATP A2, and HRP C, at pH 4–8, under conditions of high peroxide and low reducing substrate concentrations. These conditions make reaction 3 rate-limiting and, therefore, distinguish well between reducing substrates. The rate of reaction with sinapic acid is very low for all three enzymes at all pH values that were investigated, thus confirming that the extra methoxy group prevents correct binding to plant peroxidases. The slightly higher rate of turnover at low pH values reflects the higher oxidation potential of the reaction intermediates cpd I and II at low pH. HRP C has very high and rather similar reactivity toward ferulic and *p*-coumaric acid, and reacts 3–7 times faster with ferulic acid than the A2 enzymes. HRP A2 reacts 3 times

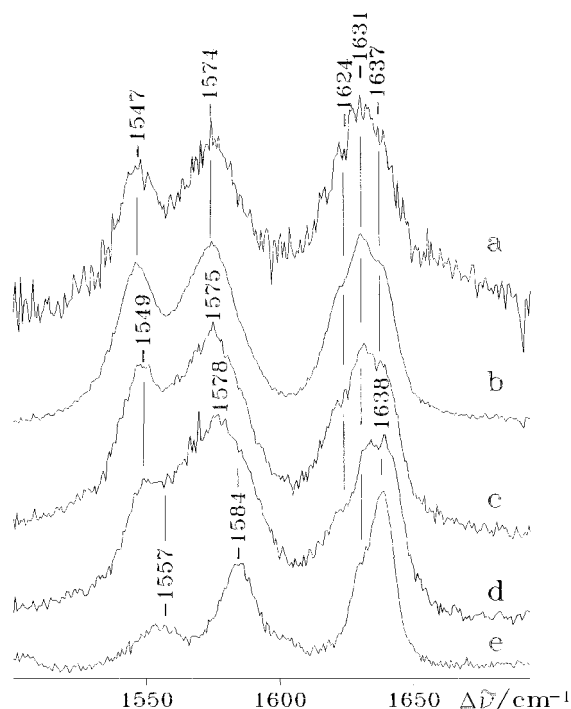


FIGURE 4: Micro RR spectra of ATP A2 crystals. (a) ATP A2 dissolved in the crystallization medium at pH 6.6, with an accumulation time of 800 s. (b) ATP A2 in bicine buffer at pH 7.5, with an accumulation time of 1800 s. (c) ATP A2 crystal form I, with an accumulation time of 960 s. (d) ATP A2 crystal form II, with an accumulation time of 2300 s. (e) ATP A2 in glycine buffer at pH 10.6, with an accumulation time of 240 s. Experimental conditions: 514.5 nm excitation, 5 cm^{-1} resolution, and 50 μW and 2.1 mW laser power in crystal and solution samples, respectively. The laser beam was moved to a new surface spot of the crystal every 60 s, and the spectra were added to give the total accumulation time.

faster and ATP A2 ~ 5 times faster with ferulic acid than with *p*-coumaric acid (discussed below).

It was unexpected that ATP A2 had only approximately 60% of the activity of HRP A2 with ferulic acid and 35% with *p*-coumaric acid, because the heme environments were indistinguishable in the spectroscopic analyses described above. To ensure that the lower activity was not a result of heme-containing but inactive ATP A2, the enzyme was freshly prepared by active site affinity chromatography on benzohydroxamic acid–agarose. Benzohydroxamic acid binding is an efficient probe for accessibility to both the hydrogen peroxide and reducing substrate binding sites (39). However, this treatment did not increase the activity of ATP A2 relative to HRP A2 (determined by reaction with ABTS).

The activities of ATP A2 and HRP A2 were analyzed further by steady-state kinetics at pH 5.0. For all five substrates, coniferyl alcohol, ferulic acid, *p*-coumaric acid, sinapic acid, and ABTS, $V/2[E]_0$ was higher for HRP A2 than for ATP A2 (Figure 5). The derived rate constant k_3 [or generally $k_2k_3/(k_2 + k_3)$] for the reaction with the electron donors was 25–200-fold smaller for sinapic acid than for ferulic and coumaric acid for both enzymes (Table 4).

For ferulic and *p*-coumaric acid, k_3 ranges from 0.25 to 4.0 $\mu\text{M}^{-1} \text{s}^{-1}$, showing that both are excellent substrates for both A2 enzymes. The steady-state analyses confirm the turnover results. ATP A2 has a significantly slower reaction with ferulic acid (58%), coniferyl alcohol (53%), and

p-coumaric acid (36%) than HRP A2. This was exactly as found for ferulic and coumaric acid in the turnover experiments. It is interesting that for coniferyl alcohol k_3 is 2-fold higher than for ferulic acid with both A2 enzymes, since these similar substrates (alcohol vs acid, Table 2) have exactly the same binding interactions with ATP A2 (20). The difference, therefore, most likely reflects the efficiency of the electron and proton transfer steps of the donor reaction, although a contribution from electrostatic repulsion during binding cannot be excluded. At pH 5.0, the acid substrate is largely on its charged and more stable form.

ABTS is seen to be a slightly slower substrate (Table 4). The simplified kinetic assumptions used here for the rate equation do not apply to ABTS. ABTS kinetics include a saturation step interpreted as a slow release of the radical product from the enzyme. The more complete kinetics equations can be found in ref 30.

The rate constant for cpd I formation, k_1 , can also be determined from steady-state kinetics (Table 4), and in principle is independent of the reducing substrate. The k_1 values at pH 5.0 for HRP A2 and ATP A2 are in good agreement considering the standard deviations. The average k_1 values for HRP A2 and ATP A2 are 1.1 and 0.82 $\mu\text{M}^{-1} \text{s}^{-1}$, respectively, using the data for the three best substrates, coniferyl alcohol, ferulic acid, and coumaric acid. Yamazaki and Nakajima (11) reported k_1 values of 1.0 $\mu\text{M}^{-1} \text{s}^{-1}$ for HRP A2 and 20 $\mu\text{M}^{-1} \text{s}^{-1}$ for HRP C. Kato et al. (40) found a k_1 value of 1.76 $\mu\text{M}^{-1} \text{s}^{-1}$ for HRP A2 at pH 5.0–8.5, and Marklund et al. (41) found a k_1 value of 1.4 $\mu\text{M}^{-1} \text{s}^{-1}$ for HRP A2 at pH 4.5.

The overall conclusion from the kinetic analyses is that the A2 peroxidases are very similar and that HRP A2 in no case reacted more than 3 times faster (coumaric acid) than ATP A2. Still, why are the enzymatic activities of HRP A2 and ATP A2 not entirely identical? Sixteen amino acid substitutions between recombinant ATP A2 and plant HRP A2 are found on the surface of the molecules (Figure 1). They do not directly affect the heme environment, as demonstrated by the spectroscopic analyses. However, the seven large glycans on the surface of HRP A2 constitute a major difference. Can they play a role either by channeling of substrate or by dampening unproductive main chain movements during substrate binding? In a series of glyco-mutants that introduced from zero to six N-linked glycans in the homologous *Coprinus cinereus* peroxidase, no significant differences were found in their specific activities (42). However, these glycans were placed far away from the active site. The observed increase in k_1 of approximately 30% for HRP A2 over that for ATP A2 is not significant, however, consistent for all substrates. It might be that the glycans at Asn147 and Asn185 channel the diffusion of H_2O_2 into the distal cavity by restricting the space available, as there are no amino acid substitutions of the polypeptide forming the distal cavity.

Coumaric acid has hydrophobic contacts to Pro69, Ile138, Pro139, and Ser140 and one hydrogen bond to Arg38. Ferulic acid and coniferyl alcohol, in addition, have contacts to Arg175 and Val178 and a second hydrogen bond from the methoxy group to Arg38 (20). All these residues are conserved between HRP A2 and ATP A2. However, several nearby residues are different between HRP A2 and ATP A2, Ala71 versus Val, Ala137 versus Ser, Phe142 versus Ile, and

Table 3: Specific Activities^a of HRP A2, ATP A2, and HRP C toward Monolignic Acids at 25 °C

pH	HRP A2 (s ⁻¹)			ATP A2 (s ⁻¹)			HRP C (s ⁻¹)		
	ferulic acid	coumaric acid	sinapic acid	ferulic acid	coumaric acid	sinapic acid	ferulic acid	coumaric acid	sinapic acid
4	645 ± 12	212 ± 18	12 ± 0.9	464 ± 17	65 ± 6	2.1 ± 0.1	3277 ± 142	1536 ± 98	14 ± 1.5
5	681 ± 21	243 ± 21	10 ± 0.8	397 ± 22	84 ± 4	2.0 ± 0.3	2506 ± 112	1997 ± 1129	5 ± 0.1
6	581 ± 11	207 ± 11	6 ± 0.3	363 ± 8	83 ± 7	1.6 ± 0.2	1817 ± 87	1947 ± 97	4 ± 0.3
7	499 ± 7	165 ± 8	4 ± 0.2	303 ± 13	48 ± 3	1.3 ± 0.1	1429 ± 57	1522 ± 42	3 ± 0.2
8	199 ± 13	63 ± 8	2 ± 0.2	92 ± 7	16 ± 3	0.8 ± 0.1	1009 ± 63	999 ± 45	3 ± 0.2

^a The turnover number ($V/[E]_0$) was measured at 500 μM H_2O_2 , at 136 μM monolignic acid, and at an enzyme concentration between 1 and 15 nM.

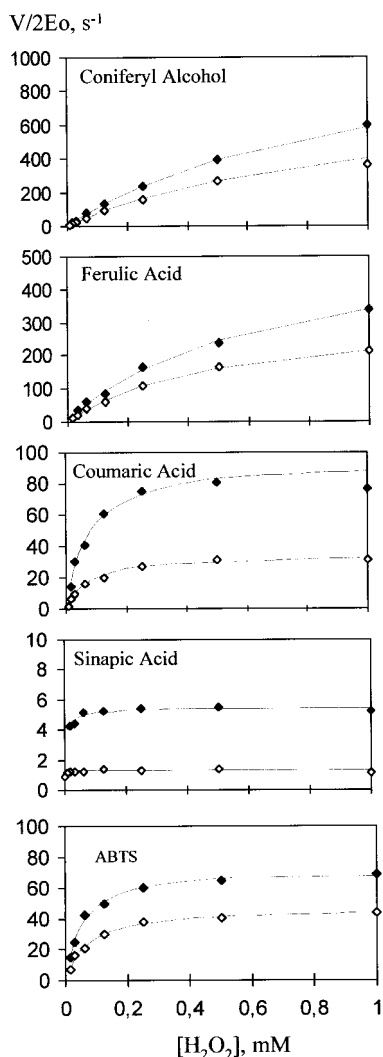


FIGURE 5: Steady-state analyses of ATP A2 (\diamond) and HRP A2 (\blacklozenge) reactions at 25 °C and pH 5.0. The velocity is shown as a function of hydrogen peroxide concentration, at 136 μM reducing substrate. The derived rate constants k_1 and k_3 are shown in Table 4.

Gly144 versus Ser. Besides, Asn147, Asn185, and Asn211 are glycosylated in HRP A2 but not in the recombinant ATP A2 (Figure 1). These differences are likely to directly influence the binding and release of large substrates and products, for example, ABTS (structure shown in Table 2). Since HRP A2 showed a faster reaction with ABTS, the glycans are not giving rise to steric hindrance. The higher rate of reaction of ferulic acid compared with that of coumaric acid seems to be related to the more specific binding of this substrate. Therefore, better and maybe faster binding of electron donors might also be the major reason

Table 4: Apparent Rate Constants for HRP A2 and ATP A2 Derived from Steady-State Experiments at 25 °C and pH 5.0

	HRPA2		ATPA2	
	k_1 ($\mu\text{M}^{-1} \text{s}^{-1}$)	k_3 ($\mu\text{M}^{-1} \text{s}^{-1}$)	k_1 ($\mu\text{M}^{-1} \text{s}^{-1}$)	k_3 ($\mu\text{M}^{-1} \text{s}^{-1}$)
coniferyl alcohol	1.2 ± 0.1	8.7 ± 0.3	0.86 ± 0.12	4.6 ± 0.2
ferulic acid	0.89 ± 0.18	4.0 ± 0.2	0.67 ± 0.10	2.3 ± 0.1
coumaric acid	1.3 ± 0.2	0.70 ± 0.03	0.92 ± 0.14	0.25 ± 0.01
sinapic acid	1.1 ± 0.6	0.04 ± 0.02	0.89 ± 0.25	0.01 ± 0.004
ABTS	1.3 ± 0.1	0.53 ± 0.01	0.68 ± 0.08	0.34 ± 0.01

for the differential reactivity of HRP A2 and ATP A2. Again, the glycans might assist in guiding, and Phe142 in catching, an electron donor at the binding site. In fact, substituting Phe142 with Ala in HRP C showed that Phe142 is an important, although indirect, determinant of aromatic donor binding and dynamics (43). We propose that the bulky glycan attached at Asn147 might strengthen the binding of both ferulic and coumaric acid by dampening the movement of the main chain of binding residues 138–140, and that this is a major effect. Glycosylated Asn185 might have a similar, additional effect on the binding by residues 175 and 178, in the case of ferulic acid and coniferyl alcohol. The decreased dynamic fluctuations caused by a large glycan have been demonstrated by an NMR study comparing the dynamics of nonglycosylated ribonuclease A and various glycoforms of ribonuclease B by amide proton exchange (44).

CONCLUSIONS

This study of plant anionic horseradish peroxidase HRP A2 and the orthologous *Arabidopsis* peroxidase ATP A2, produced recombinantly in *E. coli*, provides an example of how spectroscopy, crystallography, and enzyme kinetics might complement each other. The published crystal structure of ATP A2 was obtained after flash freezing to 100 K, and was overall very similar to that of HRP C (20). However, the distal cavity of ATP A2 contained a water moiety only 2.1 Å from the heme iron. A ligand this close to the heme iron could give rise to a mixture of high and low spins, and impede activity. The present spectroscopic analyses of ATP A2 at room temperature demonstrated a five-coordinated peroxidase heme iron with the same coordination pattern previously described for other class III plant peroxidases. New crystallographic data collected at room temperature indicated that the average Fe–water distance was increased, in agreement with the spectroscopic results. Hence, these data demonstrate that the location of a water molecule, which might be important for reactivity, could be different at low temperatures and not representative of the active state of the protein under physiological conditions. The spectroscopic analyses expanded the crystallographic picture and demon-

strated an unusual flexibility of the distal side of ATP A2 by showing (i) that two single crystals at room temperature were similar but not entirely identical in heme coordination and (ii) that lowering the temperature of the A2 enzymes in solution induces the formation of two types of low-spin hemes, bis-histidyl and hydroxyl types.

The spectroscopic comparison of HRP A2 and ATP A2 demonstrated marked and identical changes in the heme cavity over the whole range of pH stability, and on gradually lowering the temperature to 12 K. Therefore, it was expected that the enzymatic activity of the two enzymes would be identical within experimental error. The activities were indeed very similar, in particular, for the reaction with hydrogen peroxide taking place at the heme iron. However, HRP A2 had a significantly higher reactivity (up to 3-fold) than ATP A2 with coniferyl alcohol, ferulic acid, *p*-coumaric acid, and ABTS (Table 3). We propose that substitutions, no more than one to seven residues away from the major site of substrate binding (residues 138–140), are responsible for the difference in activity. In particular, we suggest that the bulky glycan attached at Asn147 in HRP A2 contributes to substrate binding by reducing the fluctuations of the main chain around residues 138–140.

This study further demonstrated that sinapic acid is a poor substrate for plant peroxidases whereas ferulic acid or coniferyl alcohol and *p*-coumaric acid are excellent substrates for ATP A2, HRP A2, and HRP C as predicted by the docking of the lignin precursors into the high-resolution structure of ATP A2. Therefore, this work provides further experimental evidence that ATP A2 plays a central role in lignification by catalyzing the oxidative polymerization of coniferyl and coumaryl alcohol into lignin in *Arabidopsis* as previously stated (20). The mechanism of sinapyl alcohol incorporation into lignin must be different.

REFERENCES

- Shannon, L. M., Kay, E., and Lew, J. Y. (1966) *J. Biol. Chem.* 241, 2166–2172.
- Paul, K.-G., and Stigbrand, T. (1970) *Acta Chem. Scand.* 24, 3607–3617.
- Aibara, S., Kobayashi, T., and Morita, I. (1981) *J. Biochem.* 90, 489–496.
- Welinder, K. G. (1976) *FEBS Lett.* 72, 19–23.
- Smith, A. T., Santama, N., Dacey, S., Edwards, M., Bray, R. C., Thorneley, R. N. F., and Burke, J. F. (1990) *J. Biol. Chem.* 265, 2920–2932.
- Smith, A. T., and Veitch, N. C. (1998) *Curr. Opin. Chem. Biol.* 2, 269–278.
- Smulevich, G. (1998) *Biospectroscopy* 4, S3–S17.
- Veitch, N. C., and Smith, A. T. (2000) *Adv. Inorg. Chem.* 51, 107–162.
- Gajhede, M., Schuller, D. J., Henriksen, A., Smith, A. T., and Poulos, T. L. (1997) *Nat. Struct. Biol.* 4, 1032–1038.
- Henriksen, A., Smith, A. T., and Gajhede, M. (1999) *J. Biol. Chem.* 274, 35005–35011.
- Yamazaki, I., and Nakajima, R. (1986) in *Molecular and Physiological Aspects of Plant Peroxidases* (Greppin, H., Penel, C., and Gaspar, T., Eds.) pp 71–84, University of Geneva, Geneva, Switzerland.
- Hiner, A. N. P., Hernandez-Ruiz, J., Arnao, M. B., Garcia-Canovas, F., and Acosta, M. (1996) *Biotechnol. Bioeng.* 50, 655–662.
- de Ropp, J. S., Chen, Z., and La Mar, G. N. (1995) *Biochemistry* 34, 13477–13484.
- Veitch, N. C., Williams, R. J. P., Bone, N. M., Burke, J. F., and Smith, A. T. (1995) *Eur. J. Biochem.* 233, 650–658.
- Feis, A., Howes, B. D., Indiani, C., and Smulevich, G. (1998) *J. Raman Spectrosc.* 29, 933–938.
- Howes, B. D., Feis, A., Indiani, C., Marzocchi, M. P., and Smulevich, G. (2000) *J. Biol. Inorg. Chem.* 5, 227–235.
- Rasmussen, S. B. (1991) M.Sc. Thesis, University of Copenhagen, Copenhagen, Denmark.
- Harthill, J. E., and Ashford, V. A. (1992) *Biochem. Soc. Trans.* 20, 113S.
- Østergaard, L., Abelskov, A. K., Mattsson, O., and Welinder, K. G. (1996) *FEBS Lett.* 398, 243–247.
- Østergaard, L., Teilum, K., Mirza, O., Mattsson, O., Petersen, M., Welinder, K. G., Mundy, J., Gajhede, M., and Henriksen, A. (2000) *Plant Mol. Biol.* 44, 231–243.
- Studier, F. W., Rosenberg, A. H., Dunn, J. J., and Dubendorff, J. W. (1990) *Methods Enzymol.* 185, 60–89.
- Teilum, K., Østergaard, L., and Welinder, K. G. (1999) *Protein Expression Purif.* 15, 77–82.
- Reimann, L., and Schonbaum, G. R. (1978) *Methods Enzymol.* 52, 514–521.
- Sørensen, K. (1993) M.Sc. Thesis, University of Copenhagen, Copenhagen, Denmark.
- Smulevich, G., Feis, A., Indiani, C., Becucci, M., and Marzocchi, M. P. (1999) *J. Biol. Inorg. Chem.* 4, 39–47.
- Brünger, A. T., Adams, P. D., Clore, G. M., DeLano, W. L., Gros, P., Grosse-Kunstleve, R. W., Jiang, J.-S., Kuszewski, J., Nilges, M., Pannu, N. S., Read, R. J., Rice, L. M., Simonson, T., and Warren, G. L. (1998) *Acta Crystallogr. D54*, 905–921.
- Rasmussen, C. B., Dunford, H. B., and Welinder, K. G. (1995) *Biochemistry* 34, 4022–4029.
- Childs, R. E., and Bardsley, W. G. (1975) *Biochem. J.* 145, 93–103.
- Dunford, H. B. (1999) *Heme Peroxidases*, John Wiley and Sons, New York.
- Abelskov, A. K., Smith, A. T., Rasmussen, C. B., Dunford, H. B., and Welinder, K. G. (1997) *Biochemistry* 36, 9453–9463.
- Henriksen, A., Mirza, O., Indiani, C., Teilum, K., Smulevich, G., Welinder, K. G., and Gajhede, M. (2001) *Protein Sci.* 10, 108–115.
- Howes, B. D., Schiødt, C. B., Welinder, K. G., Marzocchi, M. P., Ma, J.-G., Zhang, J., Shelnutt, J. A., and Smulevich, G. (1999) *Biophys. J.* 77, 478–492.
- Tamura, M. (1971) *Biochim. Biophys. Acta* 243, 249–258.
- Indiani, C., Feis, A., Howes, B. D., Marzocchi, M. P., and Smulevich, G. (2000) *J. Inorg. Biochem.* 79, 269–274.
- Smulevich, G., Wang, Y., Mauro, J. M., Wang, J., Fishel, L. A., Kraut, J., and Spiro, T. G. (1990) *Biochemistry* 29, 7174–7180.
- Nimz, H. (1974) *Angew. Chem., Int. Ed.* 13, 313–321.
- Welinder, K. G., Mauro, J. M., and Nørskov-Lauritsen, L. (1992) *Biochem. Soc. Trans.* 20, 337–340.
- Welinder, K. G. (1992) *Curr. Opin. Struct. Biol.* 2, 388–393.
- Henriksen, A., Schuller, D. J., Meno, K., Welinder, K. G., Smith, A. T., and Gajhede, M. (1998) *Biochemistry* 37, 8054–8060.
- Kato, M., Aibara, S., Morita, Y., Nakatani, H., and Hiromi, K. (1984) *J. Biochem.* 95, 861–870.
- Marklund, S., Ohlsson, P.-I., Opara, A., and Paul, K.-G. (1974) *Biochim. Biophys. Acta* 350, 304–313.
- Tams, J. W., Vind, J., and Welinder, K. G. (1999) *Biochim. Biophys. Acta* 1432, 214–221.
- Veitch, N. C. (1995) *Biochem. Soc. Trans.* 23, 232–240.
- Rudd, P. M., Joao, H. C., Coghill, E., Fiten, P., Saunders, M. R., Oudenakker, G., and Dwek, R. A. (1994) *Biochemistry* 33, 17–22.
- Laskowski, R. A., MacArthur, M. W., Moss, D. S., and Thornton, J. M. (1993) *J. Appl. Crystallogr.* 26, 283–291.
- Rasmussen, C. B., Henriksen, A., Abelskov, A. K., Jensen, R. B., Rasmussen, S. K., Hejgaard, J., and Welinder, K. G. (1997) *Physiol. Plant.* 100, 102–110.